Numerically Stable Moment Matching for General Polynomially Parameterized Linear Systems

Ortwin Farle, and Romanus Dyczij-Edlinger, *Member, IEEE,*

***Abstract*—Nowadays, the finite element method is not only used for analyzing completed microwave structures, but is increasingly integrated into the design process, see e.g. parametric studies and automatic optimization. The systems under investigation are now considered to be parameter dependent. Typical parameters include frequency, material properties and geometry parameters. To efficiently handle such parameter dependent finite element models, parametric model order reduction has been developed. Whereas order reduction methods for single parameter systems are highly developed, numerical robustness is still a field of active research for multiple parameters. In this paper we will present a new numerically stable model order reduction method for the important case of multivariate polynomially parameterized systems. In addition we will investigate important system properties of the reduced order model, such as reciprocity, stability and passivity. These investigations enable us to develop a new projection method for preserving passivity and reciprocity, which has important advantages over existing methods, even in the single parameter case.**

***Index Terms*—Finite element methods, reduced order systems.**

I. Introduction

AMONG the various numerical electromagnetic techniques, the finite element method (FEM) is one of the most versatile in handling arbitrary material properties and geometric shapes. During a design cycle or a parametric study, a process of repeated simulation alternating with changing of the parameters is performed. Due to the large number of simulations, the high computational times often prevent a sufficiently dense sampling of parameter space. This is especially true, when multiple parameters are involved. As a possible solution to this problem, model order reduction (MOR) techniques have recently been extended from the single parameter [1] to the multiple parameter case [2], [3], [4]. Order reduction is a well established methodology in the electromagnetic community for computing fast frequency sweeps [5]. In recent times additional parameters like incidence angles [6], wire spacings [7] and material properties are considered [8]. Most modern order reduction methods are of projection type, i.e. the original full model is projected onto a low dimensional subspace of appropriate global shape functions. The proposed methods mainly differ in the choice of projection basis. They can be classified as either single-point or multipoint methods. Single-point methods are usually of moment matching type, this means the transfer function and its derivatives up to a certain order are identical for the reduced order model (ROM) and the full model in a chosen expansion point. As long as the FE system can be factorized, single-point methods are very attractive since they usually require only one matrix factorization and several matrix-vector multiplications and forward and back substitutions. Multipoint methods come along with the need for a separate matrix factorization in each expansion point, which can be extremely time consuming.

The direct computation of the moments to achieve moment-matching is with rising order increasingly ill conditioned. For single-parameter systems this problem has been solved with the advent of Krylov methods, first for linear parameterization [**?**], and finally for polynomial parameterization [9], [10]. The latter was possible by extending the notion of Krylov subspaces to higher order. The generalization of the numerically stable Krylov subspace methods from the single to the multiparameter case is up to now not fully solved. Therefore, most of the proposed methods avoid the difficulties by resorting to multipoint methods [6], where only moments of low order are considered in each expansion point. In [**?**] it is proposed to discard the mix terms and only take the terms along the coordinate axes into account. This allows the use of numerically robust single-point methods along the coordinate axes. Even though this approach may lead to good results for many practical applications, in [8], Sec. III, A. a system is presented, for which this method will certainly fail. The authors of [11] solve the problem of numerical robustness for linear parameterization by considering a superspace of the sought projection space. Its special structure allows the stable computation of a basis by using the Arnoldi algorithm. Since more projection vectors are computed than are really needed for matching the moments, this method requires additional numerical costs for ROM generation and evaluation. In [**?**], a generalization of the Arnoldi algorithm is presented. Even though this approach allows a stable computation along one parameter axis, the computation of moments along other axes still suffers from numerical cancelation. This reduces the applicability of the method to the case where the parameter space is broadband along one parameter and only minor parameter changes along other directions are considered. Another interesting approach for dealing with the numerical stability problem is given in [12]. It is shown, how the construction of the multiparameter projection basis can be reduced in the multilinear case to a sequence of properly chosen single-parameter sweeps.

In this paper we will pick up this idea and extend it to the case of multivariate polynomial parameterization. One possible way to render the application of algorithms developed for multilinear parameterization possible is to linearize the polynomial

The authors are with Lehrstuhl für Theoretische Elektrotechnik, Saarland University, Campus, D-66123, Germany (e-mail: o.farle@lte.uni-saarland.de)

Manuscript received April 19, 2005; revised January 11, 2007.

problem. With increasing polynomial degree this can lead to prohibitive memory consumption and computational costs, and therefore should be avoided. To the authors knowledge, the only method capable of directly handling polynomial systems in a numerically robust way, is the algorithm presented in [13]. Even though this method performs quite well in the vast majority of cases, it is still a kind of QR-factorization of the multivariate Krylov space, which may lead to numerical instabilities at high moment orders. The method we will present in Section V does not suffer from these restrictions, since we are able to utilize the Krylov methods developed for the univariate polynomial case. Beside the increased numerical stability, this also leads to reduced memory requirements, shorter computational times and a straight forward way of parallelization.

In Section IV we examine the resulting ROMs with regard to their stability, reciprocity and passivity. These three system properties are of vital importance if the ROMs are used in a circuit simulator. Building on this analysis we develop an order reduction approach which preserves all of these system properties. It extends existing methods [14] in a twofold way: It avoids the linearization of the system, and it allows the choice of complex expansion points.

II. Motivation and Statement of the Problem

We consider the following boundary value problem (BVP)

$$\nabla \times \mu_r^{-1} \nabla \times \boldsymbol{E} + jk_0\eta_0\sigma\boldsymbol{E} - k_0^2\varepsilon_r\boldsymbol{E} = 0 \quad \text{in } \Omega \tag{1a}$$

$$\hat{\boldsymbol{n}} \times (\boldsymbol{E} \times \hat{\boldsymbol{n}}) = 0 \quad \text{on } \Gamma_E \tag{1b}$$

$$\hat{\boldsymbol{n}} \times (\boldsymbol{H} \times \hat{\boldsymbol{n}}) = \bar{\boldsymbol{H}}_t \quad \text{on } \Gamma_H \tag{1c}$$

$$\hat{\boldsymbol{n}} \times (\boldsymbol{E} \times \hat{\boldsymbol{n}}) = Z_s \boldsymbol{H} \times \hat{\boldsymbol{n}} \quad \text{on } \Gamma_Z \tag{1d}$$

where $\Omega \subset \mathbb{R}^3$ stands for the field domain with boundary $\partial\Omega = \Gamma$. The boundary consists of three disjoint subsets $\Gamma = \Gamma_E \cup \Gamma_H \cup \Gamma_Z$. In (1), $\boldsymbol{E}$ and $\boldsymbol{H}$ denote the electric and magnetic field intensity, respectively, μ_r the relative magnetic permeability, ε_r the relative electric permittivity, σ the conductivity, k_0 and η_0 the free space wave number and characteristic impedance, respectively. For the rest of this paper we will assume real and scalar material properties. The outward pointing normal unit vector on surface Γ is given by $\hat{\boldsymbol{n}}$. In (1d), Z_s stands for a frequency independent surface impedance, which is usually used as an absorbing boundary condition (ABC) of lowest order. The imposed tangential component of the magnetic field intensity $\bar{\boldsymbol{H}}_t$ is zero, except at the feeding waveguide port $\Gamma_P \subseteq \Gamma_H$. For the sake of clarity of presentation and without loss of generality, we will restrict ourselves to one single port. At this waveguide port, we expand the tangential electric and magnetic field

$$\boldsymbol{E}_t = \sum_{\xi=1}^{\infty} V_\xi \hat{\boldsymbol{e}}_{t\xi}, \quad \boldsymbol{H}_t = \sum_{\xi=1}^{\infty} I_\xi \hat{\boldsymbol{h}}_{t\xi}, \quad V_\xi, I_\xi \in \mathbb{C} \tag{2}$$

where $\hat{\boldsymbol{e}}_{t\xi}$ and $\hat{\boldsymbol{h}}_{t\xi}$ are the transversal modal fields, satisfying

$$\int_{\Gamma_P} (\hat{\boldsymbol{e}}_{t\xi} \times \hat{\boldsymbol{h}}_{t\zeta}) \cdot \hat{\boldsymbol{n}} \,\mathrm{d}\Gamma = \begin{cases} 1 & \text{if } \xi = \zeta \\ 0 & \text{if } \xi \neq \zeta \end{cases}. \tag{3}$$

In general, the model fields $\hat{\boldsymbol{e}}_{t\xi}$ and $\hat{\boldsymbol{h}}_{t\xi}$ are frequency dependent. For the important special case of TE and TM modes, $\hat{\boldsymbol{e}}_{t\xi}$ gets frequency independent. With

$$\hat{\boldsymbol{e}}_{t\xi} = Z_w(k_0) \hat{\boldsymbol{h}}_{t\xi} \times \hat{\boldsymbol{n}} \tag{4}$$

where Z_w denotes the wave impedance, only the normalization (3) gets frequency dependent. We here propose to use an impedance formulation, since a scattering formulation [15] leads to non polynomial frequency dependence of the system matrix in the case of TE and TM modes. The projection framework of Section III can be applied to TE and TM modes because the frequency dependence of the modal fields is given by (4). For details see [16]. Nevertheless, for the rest of this paper we will restrict ourselves to TEM modes, since this drastically reduces notation overhead and avoids technicalities in the analysis of Section IV.

The output of interests, in our case the generalized impedances, are given by the output functional

$$z_{\zeta\xi} = \int_{\Gamma_P} (\boldsymbol{E}_\xi \times \hat{\boldsymbol{h}}_{t\zeta}) \cdot \hat{\boldsymbol{n}} \,\mathrm{d}\Gamma \tag{5}$$

where $\boldsymbol{E}_\xi$ is the electric field intensity due to the excitation $-\hat{\boldsymbol{h}}_{t\xi}$. We adopt the minus sign because $\hat{\boldsymbol{n}}$ is outward pointing and the usual circuit port definition employs inward flowing currents. In the discrete model, we restrict the shape and test functions at the port to a finite number of v modes. The generalized impedance matrix $\mathbf{Z} = [z_{\xi\zeta}]$ therefore represents the output functionals corresponding to all excitation and test functions. A FE discretization of (1) and (5) with $H(\mathrm{curl})$-conforming shape functions [17] results in the polynomially parameterized system

$$(\mathbf{S} + jk_0\mathbf{R} - k_0^2\mathbf{T})\mathbf{x}(k_0) = jk_0\eta_0\mathbf{B}\mathbf{i} \tag{6a}$$

$$\mathbf{v} = \mathbf{B}^T\mathbf{x}(k_0) \tag{6b}$$

where

$$S_{ik} = \int_\Omega \nabla \times \boldsymbol{w}_i \cdot \mu_r^{-1} \nabla \times \boldsymbol{w}_k \,\mathrm{d}\Omega \tag{7}$$

$$R_{ik} = \eta_0 \int_\Omega \boldsymbol{w}_i \cdot \sigma \boldsymbol{w}_k \,\mathrm{d}\Omega + \eta_0 \int_{\Gamma_Z} \hat{\boldsymbol{n}} \times \boldsymbol{w}_i \cdot \frac{1}{Z_s} \hat{\boldsymbol{n}} \times \boldsymbol{w}_k \,\mathrm{d}\Gamma \tag{8}$$

$$T_{ik} = \int_\Omega \boldsymbol{w}_i \cdot \varepsilon_r \boldsymbol{w}_k \,\mathrm{d}\Omega \tag{9}$$

$$B_{ik} = \int_{\Gamma_P} (\boldsymbol{w}_i \times \hat{\boldsymbol{h}}_k) \cdot \hat{\boldsymbol{n}} \,\mathrm{d}\Gamma = \begin{cases} 1 & \text{if } \boldsymbol{w}_i = \hat{\boldsymbol{e}}_{tk} \\ 0 & \text{else} \end{cases} \tag{10}$$

$$\mathbf{i} = \begin{bmatrix} -I_1 & \dots & -I_v \end{bmatrix}^T \tag{11}$$

$$\mathbf{v} = \begin{bmatrix} V_1 & \dots & V_v \end{bmatrix}^T. \tag{12}$$

The corresponding impedance matrix $\mathbf{Z}$ is given by

$$\mathbf{Z} = jk_0\eta_0\mathbf{B}^T(\mathbf{S} + jk_0\mathbf{R} - k_0^2\mathbf{T})^{-1}\mathbf{B}. \tag{13}$$

From $\mathbf{Z}$, the computation of other network matrices like the scattering matrix $\mathbf{S}$ is straight forward.

Beside the wavenumber, we now introduce additional parameters. On a subdomain $\Omega_\varepsilon \subset \Omega$, the value of the relative electric permittivity is given as a function of a parameter s_1

$$\varepsilon_r = \overline{\varepsilon_r}(1 + s_1). \tag{14}$$

On another subdomain $\Omega_\mu \subset \Omega$ we vary the permeability according to

$$\mu_r^{-1} = \overline{\mu_r^{-1}}(1 + s_2). \tag{15}$$

In (14) und (15), the overlined quantities denote nominal values. For $\Omega_\varepsilon \cap \Omega_\mu = \emptyset$ we get the multivariate polynomially parameterized system

$$\begin{aligned}(\mathbf{S} + s_2\mathbf{S}_\mu + jk_0\mathbf{R} - k_0^2\mathbf{T} - s_1k_0^2\mathbf{T}_\varepsilon)\mathbf{x}(k_0, s_1, s_2)& \\ = jk_0\eta_0\mathbf{Bi}& \quad (16a)\\ \mathbf{v} = \mathbf{B}^T\mathbf{x}(k_0, s_1, s_2).& \quad (16b)\end{aligned}$$

III. Projection Spaces for Moment Matching

We consider linear systems parameterized by polynomials of maximum degree M in m scalar parameters $s_1, s_2, \ldots, s_m \in \mathbb{C}$. In general, such a system $\Sigma(\mathbf{s})$ takes the form

$$\left(\sum_{|\alpha|=0}^{|\alpha|\leq M} \mathbf{s}^\alpha \mathbf{A}_\alpha\right)\mathbf{x}(\mathbf{s}) = \left(\sum_{|\alpha|=0}^{|\alpha|\leq M} \mathbf{s}^\alpha \mathbf{b}_\alpha\right)u(\mathbf{s}), \tag{17a}$$

$$y(\mathbf{s}) = \left(\sum_{|\alpha|=0}^{|\alpha|\leq M} \mathbf{s}^\alpha \mathbf{c}_\alpha^H\right)\mathbf{x}(\mathbf{s}), \tag{17b}$$

where $\mathbf{A}_\alpha \in \mathbb{C}^{N\times N}$, $\mathbf{x}, \mathbf{b}_\alpha, \mathbf{c}_\alpha \in \mathbb{C}^N$, and $\alpha = (\alpha_1, \alpha_2, \ldots, \alpha_m)$ is a multi-index with $\alpha_i \geq 0$. We use the following conventions:

$$|\alpha| = \sum_{i=1}^m \alpha_i, \quad \alpha! = \prod_{i=1}^m \alpha_i!, \quad \mathbf{s}^\alpha = \prod_{i=1}^m s_i^{\alpha_i}, \tag{18}$$

$$D^\alpha = \frac{\partial^{|\alpha|}}{\partial s_1^{\alpha_1}\ldots\partial s_m^{\alpha_m}}, \tag{19}$$

$$\mathbf{x}_\alpha = \mathbf{0} \quad \text{if } \exists i \in \{1, \ldots, m\} : \alpha_i < 0, \tag{20}$$

$$\mathbf{s} = \begin{bmatrix} s_1 & s_2 & \ldots & s_m \end{bmatrix}^T. \tag{21}$$

The *Taylor series* of the transfer function $H(\mathbf{s})$ about an expansion point $\mathbf{s}_0$ is defined by

$$H(\mathbf{s}) = \sum_{|\alpha|=0}^\infty \underbrace{\frac{1}{\alpha!}D^\alpha H(\mathbf{s})\big|_{\mathbf{s}=\mathbf{s}_0}}_{m_\alpha(\mathbf{s}_0)}(\mathbf{s}-\mathbf{s}_0)^\alpha \tag{22}$$

and the coefficient of $(\mathbf{s}-\mathbf{s}_0)^\alpha$ is called *moment* $m_\alpha(\mathbf{s}_0)$. Solving (17a) for $\mathbf{x}$ and plugging the result into (17b), we obtain for the transfer function $H(\mathbf{s}) = y(\mathbf{s})/u(\mathbf{s})$ the expression

$$H(\mathbf{s}) = \left(\sum_{|\alpha|=0}^{|\alpha|\leq M} \mathbf{s}^\alpha \mathbf{c}_\alpha^H\right)\left(\sum_{|\alpha|=0}^{|\alpha|\leq M} \mathbf{s}^\alpha \mathbf{A}_\alpha\right)^{-1}\left(\sum_{|\alpha|=0}^{|\alpha|\leq M} \mathbf{s}^\alpha \mathbf{b}_\alpha\right). \tag{23}$$

A *projection-based reduced-order model* (ROM) of (17) is defined by:

$$\left(\sum_{|\alpha|=0}^{|\alpha|\leq M} \mathbf{s}^\alpha \tilde{\mathbf{A}}_\alpha\right)\tilde{\mathbf{x}} = \left(\sum_{|\alpha|=0}^{|\alpha|\leq M} \mathbf{s}^\alpha \tilde{\mathbf{b}}_\alpha\right)u \tag{24a}$$

$$y = \left(\sum_{|\alpha|=0}^{|\alpha|\leq M} \mathbf{s}^\alpha \tilde{\mathbf{c}}_\alpha^H\right)\tilde{\mathbf{x}} \tag{24b}$$

wherein $\tilde{\mathbf{A}}_\alpha$, $\tilde{\mathbf{b}}_\alpha$, and $\tilde{\mathbf{c}}_\alpha$ are given by

$$\tilde{\mathbf{A}}_\alpha := \mathbf{W}^H\mathbf{A}_\alpha\mathbf{V} \quad \tilde{\mathbf{b}}_\alpha := \mathbf{W}^H\mathbf{b}_\alpha \quad \tilde{\mathbf{c}}_\alpha := \mathbf{V}^H\mathbf{c}_\alpha \tag{25}$$

with $\mathbf{W}, \mathbf{V} \in \mathbb{C}^{N\times n}$ and $n \ll N$.

For the rest of this section, we assume without loss of generality $u = 1$. Greek letters always stand for multi-indices of dimension N. By expanding $\mathbf{x}$ in (17a) in a Taylor series, we obtain

$$\mathbf{x}(\mathbf{s}) = \sum_{|\beta|=0}^\infty \mathbf{x}_\beta \mathbf{s}^\beta, \tag{26}$$

where $\mathbf{x}_\beta$ are are recursively defined by

$$\mathbf{x}_\beta = \mathbf{A}_{\alpha=0}^{-1}\left(\mathbf{b}_\beta - \sum_{|\alpha|=1}^{|\alpha|\leq M} \mathbf{A}_\alpha \mathbf{x}_{\beta-\alpha}\right). \tag{27}$$

The number of vectors $\mathbf{x}_\beta$ with $|\beta| \leq q$ is given by

$$D_q = \sum_{k=0}^q \binom{k+m-1}{k}. \tag{28}$$

Choosing a projection matrix $\mathbf{V}$, such that

$$\operatorname{colsp}\{\mathbf{V}\} = \operatorname{span}\{\mathbf{x}_\beta\} \tag{29}$$

with $|\beta| \leq q$, results in a ROM matching the moments $m_\beta(\mathbf{s} = \mathbf{0})$ of the original model [18].

Similar to the single parameter case, the degree of matching moments can be doubled by choosing the projection matrix $\mathbf{W}$, such that its column vectors constitute a basis of the linear hull of the Taylor coefficients of the *transposed system*

$$\left(\sum_{|\alpha|=0}^{|\alpha|\leq M} \mathbf{s}^\alpha \mathbf{A}_\alpha^T\right)\mathbf{x}'(\mathbf{s}) = \left(\sum_{|\alpha|=0}^{|\alpha|\leq M} \mathbf{s}^\alpha \overline{\mathbf{c}}_\alpha\right)u(\mathbf{s}), \tag{30a}$$

$$y(\mathbf{s}) = \left(\sum_{|\alpha|=0}^{|\alpha|\leq M} \mathbf{s}^\alpha \overline{\mathbf{b}}_\alpha^H\right)\mathbf{x}'(\mathbf{s}). \tag{30b}$$

In (30), $\overline{x}$ denotes the conjugate complex of x. A detailed proof of this moment matching property can be found in [18]. Up to now, we have only considered the single-input, single-output (SISO) case. The extension to the multi-input, multi-output (MIMO) case is straight forward by employing the block version of (27) [18]. Since $\mathbf{S}$ in (16) is singular, we have to choose an expansion point $\mathbf{s}_0 = \mathbf{0}$. Substituting $\mathbf{s} = \mathbf{s}_0 + \Delta\mathbf{s}$ into (17), we still arrive at a general polynomially parameterized system in $\Delta\mathbf{s}$, for which the theory presented so far is valid.

IV. System properties

In this section we will analyze projection based ROMs of (16) according to their reciprocity, stability and passivity.

Theorem IV.1. *A ROM of* (16) *preserves the* reciprocity *of the original model, if* $\mathbf{W} = \overline{\mathbf{V}}$*, where* $\overline{\mathbf{V}}$ *is the complex conjugate of* $\mathbf{V}$.

Proof: We first have to proof the reciprocity of the original model (16), i.e. we have to show that the transfer function is symmetric. From (16) we get

$$\mathbf{H}(k_0, s_1, s_2) = jk_0\eta_0\mathbf{B}^T(\mathbf{S} + s_2\mathbf{S}_\mu + jk_0\mathbf{R} - k_0^2\mathbf{T} - s_1k_0^2\mathbf{T}_\varepsilon)\mathbf{B}. \tag{31}$$

Since $\mathbf{S}$, $\mathbf{S}_\mu$, $\mathbf{R}$, $\mathbf{T}$ and $\mathbf{T}_\varepsilon$ are symmetric matrices, we can immediately follow the reciprocity. A projection with $\mathbf{W} = \overline{\mathbf{V}}$ corresponds to $\tilde{\mathbf{A}}_\alpha = \mathbf{V}^T\mathbf{A}_\alpha\mathbf{V}$ which clearly preserves symmetry. ∎

According to Section III a projection with $\mathbf{W} = \overline{\mathbf{V}}$ also doubles the number of matching moments.

With the introduction of the scaled complex frequency $s = jk_0$, the transfer function reads as

$$\mathbf{H}(s, s_1, s_2) = s\eta_0\mathbf{B}^T(\mathbf{S} + s_2\mathbf{S}_\mu + s\mathbf{R} + s^2\mathbf{T} + s_1s^2\mathbf{T}_\varepsilon)\mathbf{B}. \tag{32}$$

Theorem IV.2. *A ROM of* (16) *preserves the* stability *of the original model, if* $\mathbf{W} = \mathbf{V}$.

Proof: We first have to prove the stability of the original model, i.e. we have to show that the poles of transfer function (32) have negative real part. The poles correspond to the eigenvalues of the real quadratic eigenvalue problem

$$(\mathbf{A}_0 + s\mathbf{A}_1 + s^2\mathbf{A}_2)\mathbf{x} = \mathbf{0} \tag{33}$$

where

$$\mathbf{A}_0 = \mathbf{S} + s_2\mathbf{S}_\mu \qquad \mathbf{A}_1 = \mathbf{R} \qquad \mathbf{A}_2 = \mathbf{T} + s_1\mathbf{T}_\varepsilon. \tag{34}$$

Since $\mathbf{S}_\mu$ and $\mathbf{T}_\varepsilon$ are submatrices of $\mathbf{S}$ and $\mathbf{T}$, respectively, the matrices $\mathbf{S} + s_2\mathbf{S}_\mu$ and $\mathbf{T} + s_1\mathbf{T}_\varepsilon$ remain positive (semi-) definite for reasonable choices of s_1 and s_2. Reasonable here means $\varepsilon_r \geq 1$ and $\mu_r \geq 1$. In [19] it is shown that the eigenvalues of (34) have negative real part if $\mathbf{R} \neq \mathbf{0}$. For $\mathbf{R} = \mathbf{0}$, the eigenvalues lie on the imaginary axis, and therefore the original system is not stable. Since a projection with $\mathbf{W} = \mathbf{V}$ is a congruence transformation and so preserves positive (semi-) definiteness of matrices, we can immediately follow the stability of the ROM. ∎

Theorem IV.3. *A ROM of* (16) *preserves the* passivity *of the original model, if* $\mathbf{W} = \mathbf{V}$.

Proof: Like in the proof of Theorem IV.2, we first have to prove the passivity of the original model. System (16) is passive if it does not create energy, i.e.

$$\mathrm{Re}\{\mathbf{i}^H\mathbf{v}\} \geq 0. \tag{35}$$

Under the assumption of existence of $\mathbf{Z}$, we can use the relation $\mathbf{v} = \mathbf{Z}\mathbf{i}$ and arrive at the equivalent condition

$$\mathbf{i}^H(\mathbf{Z} + \mathbf{Z}^H)\mathbf{i} \geq 0. \tag{36}$$

The impedance matrix of (16) is given by

$$\mathbf{Z} = jk_0\eta_0\mathbf{B}^T(\mathbf{S} + s_2\mathbf{S}_\mu + jk_0\mathbf{R} - k_0^2\mathbf{T} + s_1s^2\mathbf{T}_\varepsilon)^{-1}\mathbf{B}. \tag{37}$$

Following the same argumentation as in the proof of Theorem IV.2 on the reasonable parameter ranges of s_1 and s_2, we can conclude that the impedance matrix of (16) is of the form

$$\mathbf{Z}(k_0) = jk_0\eta_0\mathbf{B}^T(\mathbf{S}' + jk_0\mathbf{R} - k_0^2\mathbf{T}')^{-1}\mathbf{B} \tag{38}$$

with positive (semi-) definite matrices $\mathbf{S}'$ and $\mathbf{T}'$. Plugging (38) into (36), we arrive at

$$\begin{aligned}
&\mathbf{i}^H(\mathbf{Z} + \mathbf{Z}^H)\mathbf{i} \\
&\quad= \mathbf{i}^H\left(jk_0\eta_0\mathbf{B}^T(\mathbf{S}' + jk_0\mathbf{R} - k_0^2\mathbf{T}')^{-1}\mathbf{B} - \right. \\
&\qquad \left. jk_0\eta_0\mathbf{B}^T(\mathbf{S}' + jk_0\mathbf{R} - k_0^2\mathbf{T}')^{-H}\mathbf{B}\right)\mathbf{i} \\
&\quad= jk_0\eta_0\mathbf{i}^H\mathbf{B}^T(\mathbf{S}' + jk_0\mathbf{R} - k_0^2\mathbf{T}')^{-1} \\
&\qquad \left((\mathbf{S}' + jk_0\mathbf{R} - k_0^2\mathbf{T}')^H - (\mathbf{S}' + jk_0\mathbf{R} - k_0^2\mathbf{T}')\right) \\
&\qquad (\mathbf{S}' + jk_0\mathbf{R} - k_0^2\mathbf{T}')^{-H}\mathbf{B}\mathbf{i}
\end{aligned} \tag{39}$$

Setting $\mathbf{w} = (\mathbf{S}' + jk_0\mathbf{R} - k_0^2\mathbf{T}')^{-H}\mathbf{B}\mathbf{i}$ yields

$$\begin{aligned}
\mathbf{i}^H(\mathbf{Z} + \mathbf{Z}^H)\mathbf{i} &= jk_0\eta_0\mathbf{w}^H\left(-2jk_0\mathbf{R}\right)\mathbf{w} \\
&= 2k_0^2\eta_0\mathbf{w}^H\mathbf{R}\mathbf{w} \geq 0.
\end{aligned} \tag{40}$$

The passivity proof rests on the hermitian structure of $\mathbf{S}'$, $\mathbf{R}$, $\mathbf{T}'$ and the positive semi-definiteness of $\mathbf{R}$. Since these properties are preserved by a projection with $\mathbf{W} = \mathbf{V}$, we can conclude that the resulting ROM is also passive. ∎

In view of Theorem IV.1 on one side and Theorems IV.2 and IV.3 on the other side, it seems that one has to choose whether to double the number of matching moments and preserve reciprocity or to preserve stability and passivity of the model. According to Section III, to get a moment-matching ROM, the projection matrix has to satisfy condition (29). It is still fulfilled if we choose a projection matrix $\mathbf{V}'$ with

$$\mathbf{V}' = \left[\begin{array}{cccccc} \mathrm{Re}\{\mathbf{v}_1\} & \dots & \mathrm{Re}\{\mathbf{v}_n\} & \mathrm{Im}\{\mathbf{v}_1\} & \dots & \mathrm{Im}\{\mathbf{v}_n\} \end{array}\right] \tag{41}$$

where $\mathbf{v}_i$ denotes the i-th column vector of $\mathbf{V}$. Now that $\mathbf{V}'$ is real, a projection with $\mathbf{W}' = \mathbf{V}' = \overline{\mathbf{V}'}$ preserves the symmetric (semi-) positive structure of the system matrices in (16) and therefore reciprocity, stability and passivity. Additionally, $2n$ moments are matched.

The standard approach of preserving passivity in the single-parameter case is the use of one-sided projections $\mathbf{W} = \mathbf{V}$ [20], [21]. As shown in Theorem IV.3 this also preserves passivity in the multi-parameter case, but destroys the reciprocity of the original model. Additionally, compared to our proposed method, the order of matching moments is halved. This is especially important when multiple parameters are considered, since according to (28) a doubling of matching moment order, requires more than a doubling of the size of the projection basis, when using one-sided methods. In [14] a methodology for preserving passivity and reciprocity is presented. It is based on a linearization of the polynomially parameterized model, which results in an increase in model dimension N, and therefore higher numerical costs. Perhaps more important, this approach is restricted to the choice of real expansion points. For FE models of electromagnetic structures, this often leads to insufficient ROM accuracy or high ROM dimension n.

V. Numerically Stable Computation of Projection Spaces

According to Section III, to get a ROM of moment matching type, the column vectors of the projection space has to span the linear hull of multivariate Taylor coefficients. Without loss of generality we consider (27). Representation (26) implies, that for $\epsilon \in \mathbb{C}$ and $\mathbf{p} \in \mathbb{C}^m$, the r-th derivative of $\mathbf{x}(\mathbf{s})$ in direction $\mathbf{p}$ is given by

$$\left.\frac{\mathrm{d}^r \mathbf{x}(\epsilon \mathbf{p})}{\mathrm{d}\epsilon^r}\right|_{\epsilon=0} = r! \sum_{|\beta|=r} \mathbf{x}_\beta \mathbf{p}^\beta. \tag{42}$$

It is important to notice that the right hand side of (42) is a homogeneous polynomial in $\mathbf{p}$. The left side corresponds to the r-th derivative of the solution vector of the univariat parameterized linear system of equations

$$\left(\sum_{|\alpha|=0}^{|\alpha|\leq M} \epsilon^{|\alpha|} \mathbf{p}^\alpha \mathbf{A}_\alpha\right) \mathbf{x}(\mathbf{s}) = \sum_{|\alpha|=0}^{|\alpha|\leq M} \epsilon^{|\alpha|} \mathbf{p}^\alpha \mathbf{b}_\alpha, \tag{43}$$

where ϵ is the parameter.

We define the *contraction* $\Sigma(\mathbf{s})\big|_{\mathbf{p}}$ of the multivariate polynomially parameterized system (17) in a point $\mathbf{p} \in \mathbb{C}^m$ of the parameter space to be the single parameter system

$$\left(\sum_{i=0}^{i\leq M} \epsilon^i \mathbf{A}_i\right) \mathbf{x}(\epsilon) = \sum_{i=0}^{i\leq M} \epsilon^i \mathbf{b}_m \tag{44a}$$

$$y(\epsilon) = \sum_{i=0}^{i\leq M} \epsilon^i \mathbf{c}_i^H \mathbf{x}(\epsilon) \tag{44b}$$

where

$$\mathbf{A}_i = \sum_{|\alpha|=i} \mathbf{p}^\alpha \mathbf{A}_\alpha, \quad \mathbf{b}_i = \sum_{|\alpha|=i} \mathbf{p}^\alpha \mathbf{b}_\alpha, \quad \mathbf{c}_i = \sum_{|\alpha|=i} \mathbf{p}^\alpha \mathbf{c}_\alpha. \tag{45}$$

A. Reduction to single parameter systems

We now relate the space spanned by (27) to the Taylor coefficients of a sequence of single parameter systems. In the following, we denote with $\mathcal{P}_r(\mathbf{s})$ the space of homogeneous polynomials of degree r in $\mathbf{s} \in \mathbb{C}^m$. Its dimension is given by

$$\dim \mathcal{P}_r(\mathbf{s}) = \binom{r+m-1}{r}. \tag{46}$$

In the representation

$$\mathbf{x}(\mathbf{s}) = \mathbf{x}_0 + \sum_{|\beta|=1} \mathbf{x}_\beta \mathbf{s}^\beta + \ldots + \sum_{|\beta|=m} \mathbf{x}_\beta \mathbf{s}^\beta + \ldots \tag{47}$$

of the Taylor series (26), the r-th term is a homogeneous polynomial of degree r in $\mathbf{s}$. The coefficients $\mathbf{x}_\beta$ with $|\beta| = r$ are therefore uniquely determined by the univariate Taylor coefficients of contractions (43), if the set $\mathcal{S}_r = \{\mathbf{p}_i\}$ of directions is *unisolvent* in $\mathcal{P}_r(\mathbf{s})$. So we are able to state the following theorem:

Theorem V.1. *Let $\Sigma(\mathbf{s})$ denote the multiparameter system (17), $\mathbf{x}_\beta$ its Taylor coefficients, $\Sigma(\mathbf{s})\big|_{\mathbf{p}}$ the contraction of $\Sigma(\mathbf{s})$ in direction $\mathbf{p}$, and $\mathbf{x}_r(\mathbf{p})$ the Taylor coefficient of degree r of $\Sigma(\mathbf{s})\big|_{\mathbf{p}}$. If the set of interpolation points $\mathbf{p} \in \mathcal{S}_r$ is unisolvent in $\mathcal{P}_r(\mathbf{s})$, the following statement holds:*

$$\operatorname{span}\left\{\mathbf{x}_\beta \middle| |\beta| = r\right\} = \operatorname{span}\left\{\mathbf{x}_r(\mathbf{p}) \middle| \mathbf{p} \in \mathcal{S}_r\right\}. \tag{48}$$

The importance of Theorem V.1 lies in the fact, that the computation of a basis of the linear hull of $\mathbf{x}_\beta$ can now be reduced to the computation of a basis of the linear hull of the Taylor coefficients of the single parameter systems $\Sigma(\mathbf{s})\big|_{\mathbf{p}}$. In this case, recursion (27) reduces to

$$\mathbf{x}_j = \mathbf{A}_0^{-1} \left(\mathbf{b}_j - \sum_{i=1}^{M} \mathbf{A}_i \mathbf{x}_{j-i}\right). \tag{49}$$

There exist several numerically stable algorithms to compute a basis of (49), see e.g. [9] and [10], which can now be applied to the multiparameter case.

B. Numerical Implementation

For efficiency reasons it is advantageous to utilize a *hierarchical* set of interpolation points

$$\mathcal{S}_0 \subset \mathcal{S}_1 \subset \cdots \subset \mathcal{S}_r \subset \cdots \subset \mathcal{S}_q \tag{50}$$

where each set $\mathcal{S}_r$ is unisolvent in $\mathcal{P}_r(\mathbf{s})$, and q denotes the maximum order. This approach allows the reuse of information of lower orders. In [12] the following choice is proposed

$$\mathcal{S}_r = \left\{(\gamma, q - |\gamma|) \;\middle|\; |\gamma| \leq r\right\}, \qquad r = 0, \ldots, q \tag{51}$$

where γ is a multi-index of dimension $m-1$.

To compute a numerically stable basis $\mathbf{u}_0 \ldots \mathbf{u}_q$ of the space of univariate Taylor coefficients, we use the WCAWE algorithm [9], because it can handle system matrices and right hand sides of arbitrary polynomial degree. In the following we introduce for this step the abbreviation

$$\begin{bmatrix}\mathbf{u}_0 & \ldots & \mathbf{u}_q\end{bmatrix} = \mathrm{WCAWE}\left(\Sigma(\mathbf{s})\big|_{\mathbf{p}}, q\right). \tag{52}$$

Our proposed method for computing an orthonormal basis of (29) is given in Alg. 1. In lines three and four, we consider in each interpolation point an independent single parameter model, which immediately allows a parallelization of the method. The vectors $\mathbf{u}_k(\mathbf{p})$ with $\mathbf{p} \notin \mathcal{S}_k$ are linearly dependent to the already computed basis $\mathbf{V}$ and are therefore discarded in line six. In line seven we use the modified Gram-Schmidt process (MGS) to ensure the orthonormality of matrix $\mathbf{V}$.

Algorithm 1 Proposed Algorithm - Parallel Version

```
1:  V = [ ]
2:  for ∀p ∈ S_q do
3:      Compute Σ(s)|_p according to (44a)
4:      [u_0 ... u_q] = WCAWE(Σ(s)|_p, q)
5:      for k := 0 ... q do
6:          if p ∈ S_k then
7:              v := MGS(u_k, V)
8:              V := [V, v/‖v‖]
9:          end if
10:     end for
11: end for
```

1) Efficiency improvement: Beside the factorization of the system matrix, one of the most expensive steps during the computation of the multivariate basis is the construction of $[\mathbf{u}_0, \ldots, \mathbf{u}_q]$ for each interpolation point. The dimension of the basis to be computed is given by (28). The number of vectors $\mathbf{u}_k(\mathbf{p})$ computed in Alg. 1 is

$$N_u = (q+1)\dim \mathcal{P}_q(m) = (q+1)\binom{q+m-1}{q}, \quad (53)$$

which exceeds (28). Many of the vectors with degree $r < q$ do not contribute to the basis $\mathbf{V}$. Their sole purpose is to provide the history needed by recursion (49) to compute the non redundant basis vectors of higher order.

Since the redundant vectors $\mathbf{u}_r$ are linearly dependent to the column vectors of the already computed matrix $\mathbf{V}$, they need not to be computed by the WCAWE process on the full model in each interpolation point, but can be efficiently reconstructed from the known basis vectors. This can e.g. be done by considering the ROM $\tilde{\Sigma}(\mathbf{s})$ built by projection with $\mathbf{V}$. Let $[\tilde{\mathbf{u}}_0, \ldots, \tilde{\mathbf{u}}_r]$ denote the WCAWE vectors of contraction $\tilde{\Sigma}(\mathbf{s})\big|_{\mathbf{p}}$. The WCAWE vectors of the contracted original model can be reconstructed by means of

$$\begin{bmatrix}\mathbf{u}_0 & \ldots & \mathbf{u}_r\end{bmatrix} = \mathbf{V}\begin{bmatrix}\tilde{\mathbf{u}}_0 & \ldots & \tilde{\mathbf{u}}_r\end{bmatrix}. \quad (54)$$

Since numerical costs for the WCAWE iteration on the ROM can be neglected compared to the forward back substitution on the original model, this constitutes a very efficient method for computing the linearly dependent vectors. To state the final algorithm, we first have to introduce the incremental sets of interpolation points $\tilde{\mathcal{S}}_r$:

$$\mathcal{S}_r = \tilde{\mathcal{S}}_r \oplus \mathcal{S}_{r-1}. \quad (55)$$

With this definition, the proposed method is given in Alg. 2. Note that only in line ten WCAWE vectors with dimension of the full model have to be computed. Unfortunately, the efficiency gain of this approach complicates the parallelization, since the computation of the WCAWE vectors in different interpolation points cannot be split into independent processes anymore. In [12] a similar approach was presented for the linear parameterized case.

Algorithm 2 Proposed Algorithm - Serial Version

1: $\mathbf{p} = \mathcal{S}_0$
2: Compute $\Sigma(\mathbf{s})\big|_{\mathbf{p}}$ according to (44a)
3: $\mathbf{V} = \mathrm{WCAWE}\left(\Sigma(\mathbf{s})\big|_{\mathbf{p}}, q\right)$
4: Compute $\tilde{\Sigma}(\mathbf{s})$ with $\mathbf{V}$
5: **for** $r = 1 \ldots q$ **do**
6: **for** $\forall \mathbf{p} \in \tilde{\mathcal{S}}_r$ **do**
7: Compute $\tilde{\Sigma}(\mathbf{s})\big|_{\mathbf{p}}$ according to (44a)
8: $[\tilde{\mathbf{u}}_0 \ldots \tilde{\mathbf{u}}_{r-1}] = \mathrm{WCAWE}\left(\tilde{\Sigma}(\mathbf{s})\big|_{\mathbf{p}}, r-1\right)$
9: $[\mathbf{u}_0 \ldots \mathbf{u}_{r-1}] = \mathbf{V}\,[\tilde{\mathbf{u}}_0 \ldots \tilde{\mathbf{u}}_{r-1}]$
10: $[\mathbf{u}_r \ldots \mathbf{u}_q] = \mathrm{WCAWE}\left(\Sigma(\mathbf{s})\big|_{\mathbf{p}}, [\mathbf{u}_0 \ldots \mathbf{u}_{r-1}], q\right)$
11: **for** $k = r \ldots q$ **do**
12: $\mathbf{v} := \mathrm{MGS}\,(\mathbf{u}_k, \mathbf{V})$
13: $\mathbf{V} := [\mathbf{V}, \mathbf{v}/\|\mathbf{v}\|]$
14: **end for**
15: **end for**
16: Compute $\tilde{\Sigma}(\mathbf{s})$ with $\mathbf{V}$
17: **end for**

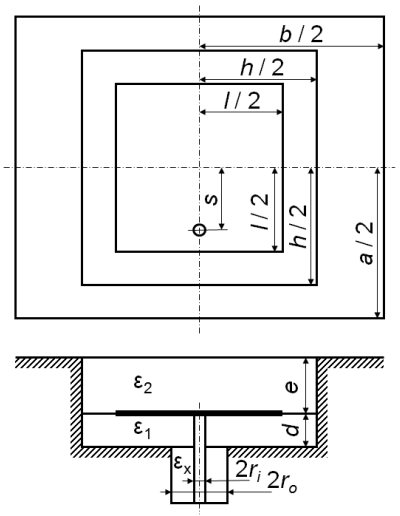

Fig. 1. Structure of patch antenna. Dimensions in mm: a=22.15, b=47.45, h=18.15, l=13.5, s=1.75, d=2.42, e=2.6, r_i=0.64, r_0=2.05.

2) Direction dependent Choice of Model Order: According to (28), the dimension of the ROM increases very strong with the considered moment order q. In the method presented so far, the order of the ROM is equal for all parameters. In many applications in contrary, parameter ranges in some parameters are wide, e.g. usually the frequency, whereas other are rather small. These different requirements on bandwidth are only inadequately fulfilled by ROMs of homogeneous order.

Since our proposed method uses single parameter systems, we can apply the error- and termination criteria developed for them, see e.g. [22] and [23, Chapter 5], to choose the order of the single parameter systems direction dependently.

VI. Numerical Examples

A. Patch Antenna

Fig. 1 shows the structure of the considered patch antenna [24]. We allow the reflection coefficient S_{11} to be a function of operation frequency f and the dielectric permittivities of the two substrate layers, ε_{r1} and ε_{r2}. The expansion point is set at $(\overline{f} = 6\ \mathrm{GHz}, \overline{\varepsilon_{r1}} = 4, \overline{\varepsilon_{r2}} = 2)$. A FE discretization with second order shape functions results in a full model with $N = 58,247$ degrees of freedom. The order of the ROM is chosen to be $q = 8$. Since we do not utilize the ROM in a circuit simulator, there is no need for preserving passivity, and we therefore use $\mathbf{W} = \overline{\mathbf{V}}$. According to (28) this results in a ROM dimension of 165. Figs. 2, 3 and 4 show the magnitude of S_{11} as a function of frequency and relative electric permittivity ε_{r1} for $\varepsilon_{r2} = 1$, $\varepsilon_{r2} = 4$ and $\varepsilon_{r2} = 7$, respectively. Note that each surface plot consists of $201 \times 201 = 40401$ model evaluations. To assess the accuracy of the new approach we present in Fig. 5 a comparison with the full FE model and an existing method [13]. Fig. 6 shows the errors of the ROMs compared to the

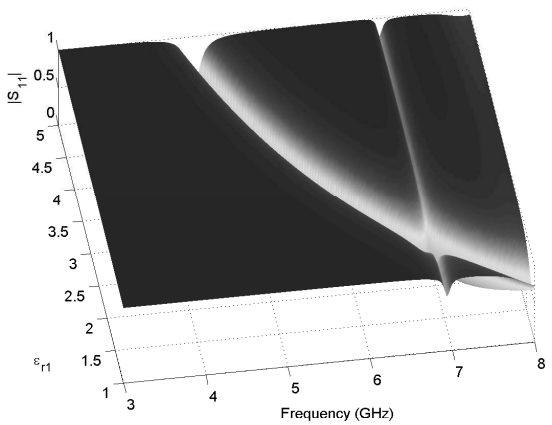

Fig. 2. Patch antenna. Magnitude of reflection coefficient at $\varepsilon_{r2} = 1$ as a function of frequency and relative electric permittivity ε_{r1}.

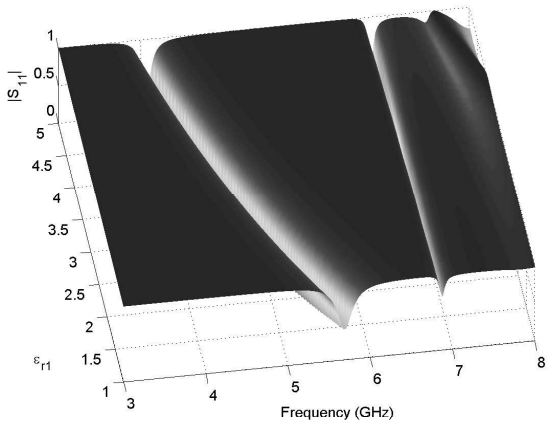

Fig. 3. Patch antenna. Magnitude of reflection coefficient at $\varepsilon_{r2} = 4$ as a function of frequency and relative electric permittivity ε_{r1}.

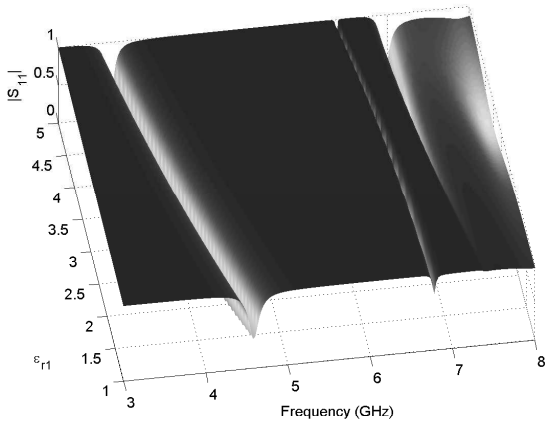

Fig. 4. Patch antenna. Magnitude of reflection coefficient at $\varepsilon_{r2} = 7$ as a function of frequency and relative electric permittivity ε_{r1}.

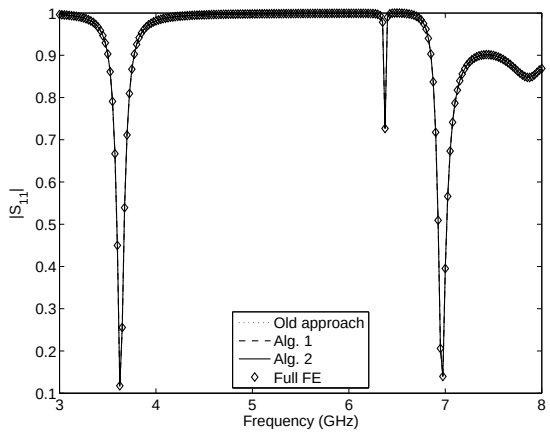

Fig. 5. Patch antenna. Magnitude of reflection coefficient as a function of frequency at $\varepsilon_{r1} = 5$, $\varepsilon_{r2} = 7$.

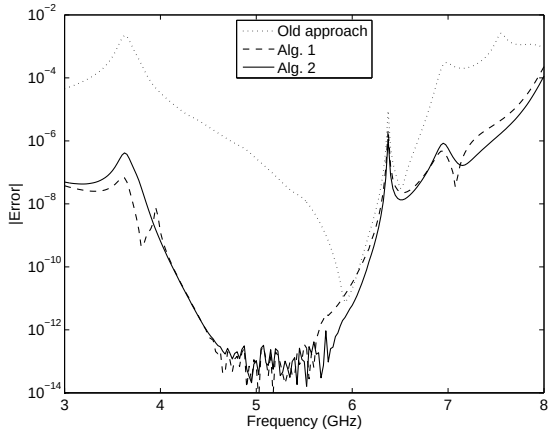

Fig. 6. Patch antenna. Magnitude of error in reflection coefficient as a function of frequency at $\varepsilon_{r1} = 5$, $\varepsilon_{r2} = 7$.

full FE model

$$|\text{Error}| = |S_{11}^{ROM} - S_{11}^{FE}|. \tag{56}$$

As can be clearly seen, the new approach leads to smaller errors in the reflection coefficient. Since the projection matrices of our proposed method and the approach presented in [13] are identical, this improvement can be contributed to an increased numerical stability. The minor differences between Alg. 1 and 2 are due to numerical noise. Table I shows the speed up attainable by using Alg. 2 for model generation. The reduction of ROM generation time between Alg. 1 and Alg 2 is approximately 30 percent. Both algorithms are substantially faster than the method of [13]. Comparing the evaluation times for ROM and full model, we see a difference of more than three orders of magnitude. The ROM can be evaluated 90 times per second. For the surface plots of Figs. 2, 3 and 4 this means a reduction of computation times from almost 13 days of the full model to approximately 9 minutes for the ROM.

B. Bandpass Filter

Fig. 7 presents a bandpass filter consisting of two dielectric resonators. We now compute the reflection coefficient as a function of frequency and relative electric permittivity of

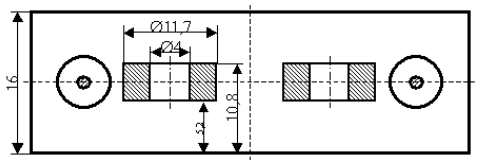

(a) Sheer plan

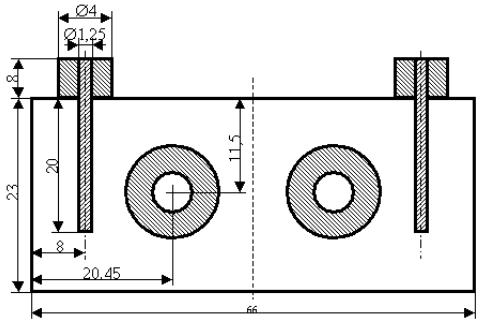

(b) Plan view

Fig. 7. Structure of bandpass filter [25].

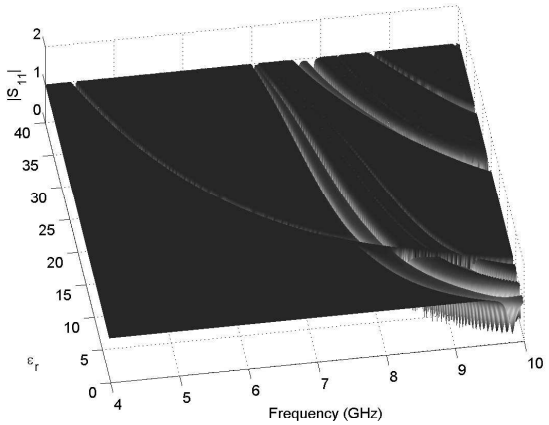

Fig. 8. Bandpass filter. Magnitude of reflection coefficient as a function of frequency and relative electric permittivity ε_r.

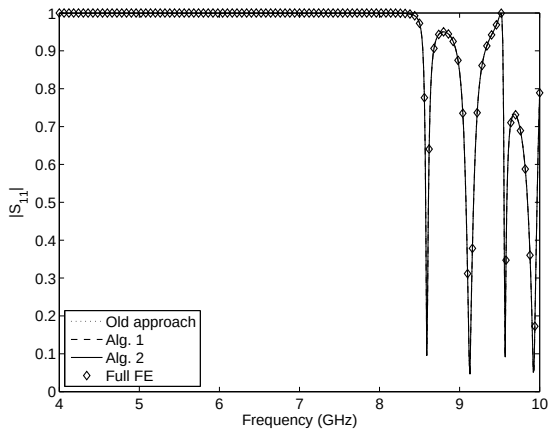

Fig. 9. Bandpass filter. Magnitude of reflection coefficient as a function of frequency at $\varepsilon_r = 5$.

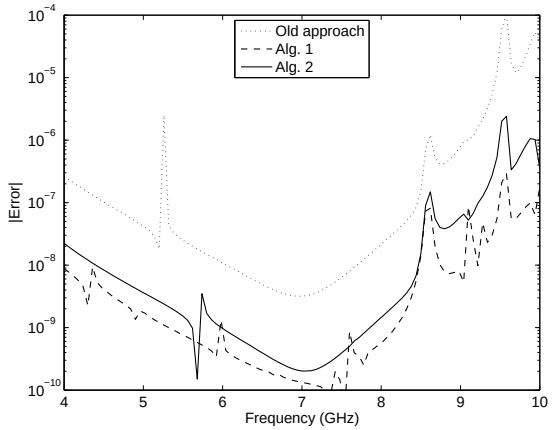

Fig. 10. Bandpass filter. Magnitude of error in reflection coefficient as a function of frequency at $\varepsilon_r = 5$.

the resonators. A FE discretization with second order shape functions gives a full model with $N = 103,848$ unknowns. We choose a ROM of order $q = 15$ with expansion point $(\overline{f} = 7 \text{ GHz}, \overline{\varepsilon_r} = 38)$. The computed response surface consisting of $301 \times 301 = 90601$ points is given in Fig. 8. To examine the accuracy of the ROM, we consider in Fig. 9 a cut through the response surface at $\varepsilon_r = 5$. Fig. 10 shows the magnitude of the error compared to the full FE model. We observe a slight increase of the error when using Alg. 2. Its error is still smaller than that of the old approach, and generation time is reduced to less than 50 percent, see Tab. I. Compared to Alg. 1, generation time is reduced by more than 30 percent. The computation time for the response surface of Fig. 8 is almost 24 days for the full model and approximately 19 minutes for the ROM.

VII. Conclusion

In this paper we presented a new algorithm for moment matching order reduction of multivariate polynomial parameterized systems. Its key features are an increased numerical robustness and reduced memory consumption compared to existing methods, in addition it allows for a straight forward parallelization. We analyzed the resulting ROMs with respect to their stability, passivity and reciprocity, and proposed a new projection method which preserves all of these properties. This new method extends existing approaches by allowing complex expansion points and avoiding the linearization of the original system.

TABLE I
Computational Data[1]

	Patch antenna	Bandpass filter
ROM Generation (s)		
Old approach	3388.57	1219.68
Algorithm 1	815.04	859.42
Algorithm 2	514.75	591.57
Model evaluation (s)		
ROM	$1.37 \cdot 10^{-2}$	$1.28 \cdot 10^{-2}$
Full FE	27.55	22.65

[1] MATLAB implementation on AMD Opteron 250 processor, 2.39 GHz.

REFERENCES

[1] L. T. Pillage and R. A. Rohrer, "Asymptotic waveform evaluation for timing analysis," *IEEE Trans. Comput.-Aided Design Integr. Circuits Syst.*, vol. 33, no. 9, pp. 352–366, Apr 1990.

[2] D. S. Weile, E. Michielssen, E. Grimme, and K. Gallivan, "A method for generating rational interpolant reduced order models of two-parameter linear systems," *Applied Mathematics Letters*, vol. 12, pp. 93–102, Jul. 1999.

[3] P. Gunupudi, R. Khazaka, and M. Nakhla, "Analysis of transmission line circuits using multidimensional model reduction techniques," *IEEE Trans. Adv. Packag.*, vol. 25, no. 2, pp. 174–180, May 2002.

[4] C. Prud'homme, D. V. Rovas, K. Veroy, L. Machiels, Y. Maday, A. Patera, and G. Turinici, "Reliable real-time solution of parameterized partial differential equations: reduced-basis output bound methods," *Journal of Fluids Engineering*, vol. 124, pp. 70–80, 2002.

[5] J. E. Bracken, D.-K. Sun, and Z. J. Cendes, "S-domain methods for simultaneous time and frequency characterization of electromagnetic devices," *IEEE Trans. Microw. Theory Tech.*, vol. 46, no. 46, pp. 1277–1290, Sep. 1998.

[6] D. S. Weile and E. Michielssen, "Analysis of frequency selective surfaces using two-parameter generalized rational Krylov model-order reduction," *IEEE Trans. Antennas Propag.*, vol. 49, pp. 1539–1549, Nov. 2001.

[7] L. Daniel, O. C. Siong, L. S. Chay, K. H. Lee, and J. White, "A multiparameter moment-matching model-reduction approach for generating geometrically parameterized interconnect performance models," *IEEE Trans. Comput.-Aided Design Integr. Circuits Syst.*, vol. 23, pp. 678–693, May 2004.

[8] O. Farle, V. Hill, P. Nickel, and R. Dyczij-Edlinger, "Multivariate finite element model order reduction for permittivity or permeability estimation," *IEEE Trans. Magn.*, vol. 42, no. 4, pp. 623–626, Apr. 2006.

[9] R. D. Slone, R. Lee, and J.-F. Lee, "Broadband model order reduction of polynomial matrix equation using single-point well-conditioned asymptotic waveform evaluation: Derivation and theory," *Int. J. Numer. Meth. Engng*, vol. 58, pp. 2325–2342, Dec. 2003.

[10] Z. Bai and Y. Su, "Dimension reduction of large-scale second-order dynamical systems via a second-order Arnoldi method," *SIAM Journal on Scientific Computing*, vol. 26, no. 5, pp. 1692–1709, 2005.

[11] L. H. Feng, E. B. Rudnyi, and J. G. Korvink, "Preserving the film coefficient as a parameter in the compact thermal model for fast electrothermal simulation," *IEEE Trans. Comput.-Aided Design Integr. Circuits Syst.*, vol. 24, no. 12, pp. 1838–1847, Dec. 2005.

[12] L. Codecasa, "A novel approach for generating boundary condition independent compact dynamic thermal networks of packages," *IEEE Transactions on Components and Packaging Technologies*, vol. 28, no. 4, pp. 593–604, Dec. 2005.

[13] O. Farle, V. Hill, P. Ingelström, and R. Dyczij-Edlinger, "Multi-parameter polynomial order reduction of linear finite element models," *Math. Comp. Model. Dyn. Sys., in press*, vol. 14, no. 5, pp. 421–434, 2008.

[14] R. W. Freund, "SPRIM: structure-preserving reduced-order interconnect macromodeling," in *Proceedings of the 2004 IEEE/ACM Int. conf. on CAD*, 2004, pp. 80–87.

[15] Z. J. Cendes and J.-F. Lee, "The transfinite element method for modeling MMIC devices," *IEEE Trans. Microw. Theory Tech.*, vol. 36, no. 12, pp. 1639–1649, Dec. 1988.

[16] J. Rubio, J. Arroyo, and J. Zapata, "SFELP-an efficient methodology for microwave circuit analysis," *IEEE Trans. Microw. Theory Tech.*, vol. 49, no. 3, pp. 509–516, Mar. 2001.

[17] P. Ingelström, "A new set of H(curl)-conforming hierarchical basis functions for tetrahedral meshes," *IEEE Trans. Microw. Theory Tech.*, vol. 54, no. 1, pp. 106–114, Jan. 2006.

[18] O. Farle, "Ordnungsreduktionsverfahren für die Finite-Elemente-Simulation parameterabhängiger passiver Mikrowellenstrukturen," Ph.D. dissertation, Saarland University, Saarbrücken, Germany, 2007.

[19] F. Tisseur and K. Meerbergen, "The quadratic eigenvalue problem," *SIAM Review*, vol. 43, no. 2, pp. 235–286, 2001.

[20] A. Odabasioglu, M. Celik, and L. Pileggi, "PRIMA: Passive reduced-order interconnect macromodeling algorithm," *IEEE Trans. Comput.-Aided Design Integr. Circuits Syst.*, vol. 17, no. 8, pp. 645–654, Aug. 1998.

[21] Y. Zhu and A. C. Cangellaris, "Finite element-based model order reduction of electromagnetic devices," *International Journal of Numerical Modelling: Electronic Networks, Devices and Fields*, vol. 15, pp. 73–92, Jan. 2002.

[22] Z. Bai, R. D. Slone, W. T. Smith, and Q. Ye, "Error bound for reduced system model by Pad´e approximation via the Lanczos process," *IEEE Trans. Comput.-Aided Design Integr. Circuits Syst.*, vol. 18, no. 2, pp. 133–141, Feb. 1999.

[23] E. Grimme, "Krylov projection methods for model reduction," Ph.D. dissertation, Coordinated-Science Laboratory, Univ. of Illinois at Urbana-Champaign, Urbana-Champaign, IL, 1997.

[24] M. A. G. de Aza, J. A. Encinar, J. Zapata, and M. Lambea, "Full-wave analysis of cavity-backed and probe-fed microstrip patch arrays by a hybrid mode-matching generalized scattering matrix and finite-element method," *IEEE Trans. Microw. Theory Tech.*, vol. 46, no. 2, pp. 234–242, Feb. 1998.

[25] J. R. Brauer and G. C. Lizalek, "Microwave filter analysis using a new 3-d finite-element modal frequency method," *IEEE Trans. Microw. Theory Tech.*, vol. 45, no. 5, pp. 810–818, May 1997.